Journal of Structural Geology, Vol. 15, No. 1, pp. 21 to 36, 1993
Printed in Great Britain

0191-8141/93 $06.00+0.00

Microstructures in feldspars from a major crustal thrust zone: the Grenville Front, Ontario, Canada

LYNN L. PRYER

Department of Geology, Erindale College, University of Toronto, Mississauga, Ontario, Canada L5L 1C6

(*Received* 17 *April* 1991; *accepted in revised form* 30 *June* 1992)

Abstract—Samples collected across the NW Grenville Front in Ontario, Canada, have been used to document the change in feldspar microstructures produced during shearing under metamorphic conditions that range from upper amphibolite to lower greenschist grade. The differential displacement across this 5 km thick section of the Grenville Front tectonic zone is at least 10 km.

At upper to mid-amphibolite conditions both plagioclase and potassium feldspars behave plastically. Grain-size reduction occurs through grain boundary migration and/or subgrain rotation and produces a core-and-mantle structure. At middle to lower amphibolite grade, grain-size reduction is accomplished through grain boundary migration. At lower amphibolite to upper greenschist grade, grain-size reduction occurs by the nucleation and growth of new grains with a different composition. The abundance of intracrystalline deformation at this grade is inversely proportional to the amount of fine-grained matrix. In ultramylonite with a high matrix to porphyroclast ratio few intracrystalline strain features occur other than ubiquitous undulatory extinction. Myrmekite is well developed on the high stress boundaries in K-feldspar.

At upper to mid-greenshist conditions, feldspars deform mainly by slip on synthetic shear fractures. Deformation twins, undulatory extinction, deformation bands and kink bands occur in plagioclase, and perthite flames and myrmekite occur principally on high stress boundaries in K-feldspar. Grain-size reduction in feldspar is accomplished through cataclasis. At middle to lower greenschist facies, deformation in feldspars is dominated by antithetic fractures. The transition from the dominance of synthetic to antithetic fractures is gradational. Below lower greenschist grade, rocks deform by pervasive cataclasis of all minerals.

INTRODUCTION

THIS paper presents the results of a petrographic study of feldspar microstructures from an area straddling the Grenville Front of Ontario, Canada. The study area is underlain by a suite of granitoids that experienced regional thrust faulting and contains a series of mylonites produced under different metamorphic conditions. An area underlain by mineralogically similar rocks deformed under different metamorphic grades, such as this, is ideally suited to observe the variety of microstructures in feldspars produced during mylonitization. These mylonites have, in general, been displaced to higher crustal levels and therefore lower metamorphic grades, decreasing the possibility of post-tectonic annealing of intricate microstructures. In some cases the superposition of microstructures produced under different conditions has occurred, but it is possible to distinguish lower grade deformation since it is always restricted to a narrower zone than that of higher grade. The underlying assumption adopted here is that the microstructures at different crustal levels within a fault zone indicate the micromechanisms active at that level (White & White 1983). It is hoped that these observations will serve as an example of feldspar microstructures produced in a natural environment that can be compared to those produced in the laboratory and will help to assess the extent to which experiments reproduce conditions in the natural world.

General geology

The Grenville Province (GP) of Canada is a major NE–SW-trending Proterozoic orogenic belt that stretches continuously from the Labrador coast in the east to the Great Lakes in the west. The Grenville Front (Derry 1950) (Fig. 1, inset), which marks the northwest boundary of the GP, is a NE-trending, SE-dipping zone of localized plastic to cataclastic shearing. In general, reverse-sense movement along the Grenville Front shear zone occurred during the Grenville orogeny (Wynne-Edwards 1972) approximately 1100 Ma ago (Stockwell 1982).

The area studied is in central Ontario, Canada (Fig. 1). It is bounded to the northwest by Huronian metasediments of the Southern Province (2200 Ma, Stockwell 1982) to the east and west by the Carlyle Township lines and to the south by Ontario Highway 637. This area is underlain by a series of NE-trending elongate intrusive and extrusive units that range in composition from granite (*sensu stricto*) to diorite. Collectively, these units form a band of igneous rocks extending geographically from the town of Killarney on Georgian Bay (K, Fig. 1) northeastward to Highway 69 near Sudbury (S, Fig. 1). The Killarney complex, which was originally called the 'Grenville Front Granites' by Frarey & Cannon (1968), has been isotopically dated between 1750 and 1500 Ma (Stockwell 1982, van Breeman & Davidson 1988). The largest and most distinctive of these units is the Bell

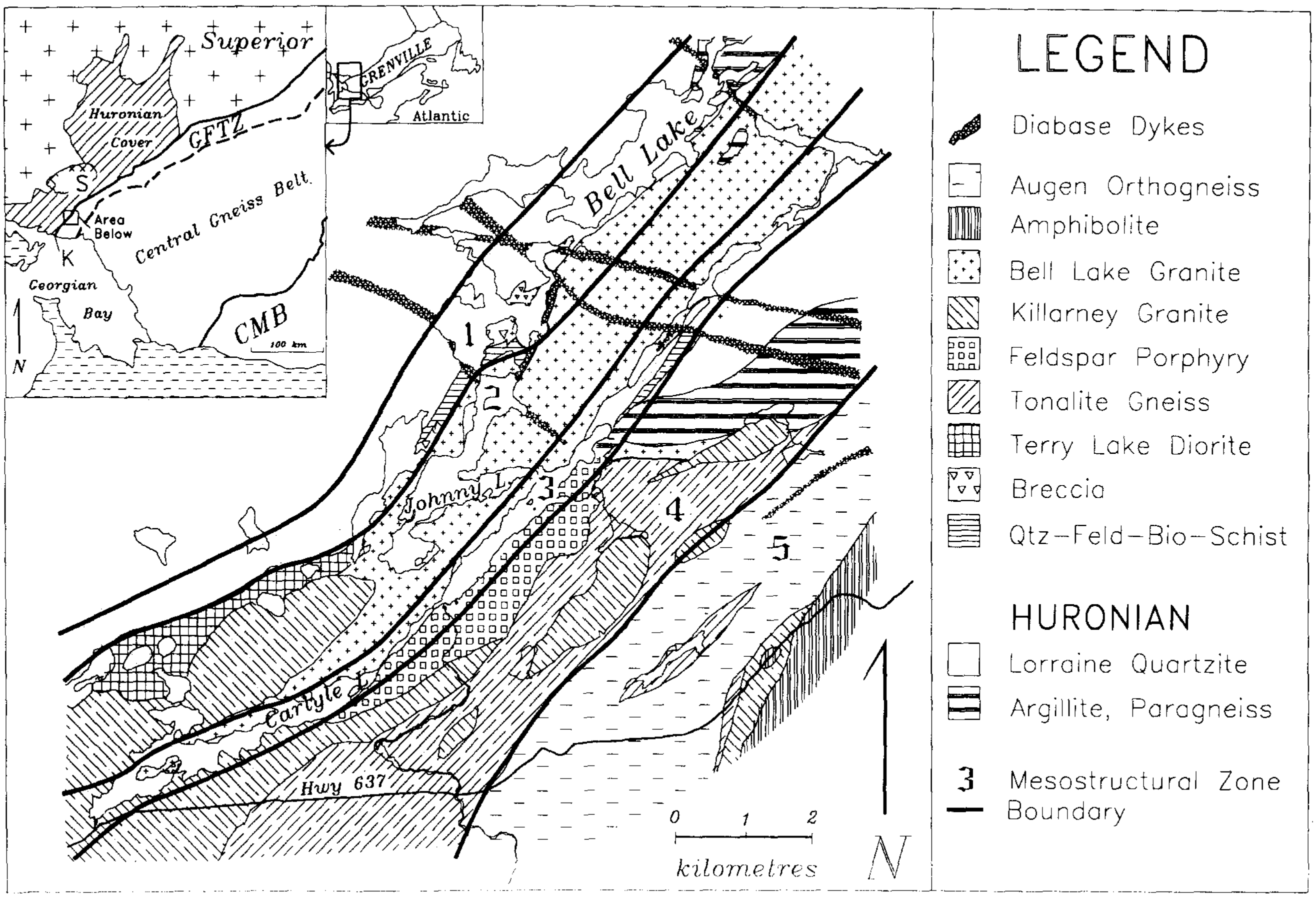

Fig. 1. Map of the Grenville Front tectonic zone in Carlyle Township and location map (inset) including lithology and mesostructural subdivisions discussed in the text. Mesostructural divisions are based on differences in both lithology and style of deformation. K—Killarney; S—Sudbury.

Lake Granite, a porphyritic granite to granodiorite that underlies approximately one-quarter of the area and transects a major anticline in the Huronian metasediments such that the fold closure is isolated and completely surrounded by the igneous complex (Fig. 1).

The manifestation of the deformation in outcrop changes from ductile to brittle as one traverses the Grenville Front tectonic zone (GFTZ; Fig. 1, inset) from the GP into the Southern Province. Foliation defined by the parallel alignment of minerals is penetrative and consistent in orientation in the GP, but becomes non-penetrative and inconsistent in the granites at the northwest limit of mapping. Mylonite zones are developed throughout the area with their consistency in orientation (Fig. 2), width and mean grain-size decreasing to cataclasite at the northwest boundary. In the Southern Province, Grenvillian age deformation is weak (e.g. La Tour & Fullagar 1986). The Johnny Lake shear zone (JLSZ; zone 3, Fig. 1) (Pryer 1985) is the largest of many mylonite zones in the area and has been taken to be the trace of the Grenville Front itself (Davidson 1986).

In this contribution, differences in lithology and mesoscopic style of deformation are used to divide the area into five zones that trend parallel to the GFTZ (Fig. 1). The general features of each of the five zones are outlined below in descending order from highest to lowest grade. The variation from mylonite to cataclasite across strike is inferred to represent an exposed crustal cross-section in which deformation features from different crustal levels are preserved. Figure 2(a) shows the attitude of all poles to foliations and mineral lineations for each zone. A summary of these data in Fig. 2(b) and Table 1 indicates that: (i) the inclination of fabric elements increases toward the northwest; (ii) lineations are essentially parallel to the true dip of the foliation; (iii) preferred orientations are stronger in the southeast; the variability in trend is much greater in the northwest; and (iv) the most pronounced change in fabric strength occurs between zones 2 and 3 (indicated by the parameter (peak $-$ E)/σ).

Zone 5 is underlain by augen orthogneiss that is most likely genetically associated with the Killarney complex. An *S–C* fabric (Lister & Snoke 1984) is well developed throughout this zone. Bands of mylonite are locally developed which are coarser grained than those in the other zones. The augen gneiss contains abundant folded and mylonitized pegmatite dykes.

Zone 4 is underlain by strongly foliated and locally mylonitic units of the Killarney complex and, in the northeast, by strongly deformed and metamorphosed Huronian sediments (i.e. the isolated fold closure). These units are intruded by numerous mutually cross-cutting pegmatite dykes that display ptygmatic folding and mylonitization indicating a long and complex history of syntectonic pegmatite intrusion and deformation.

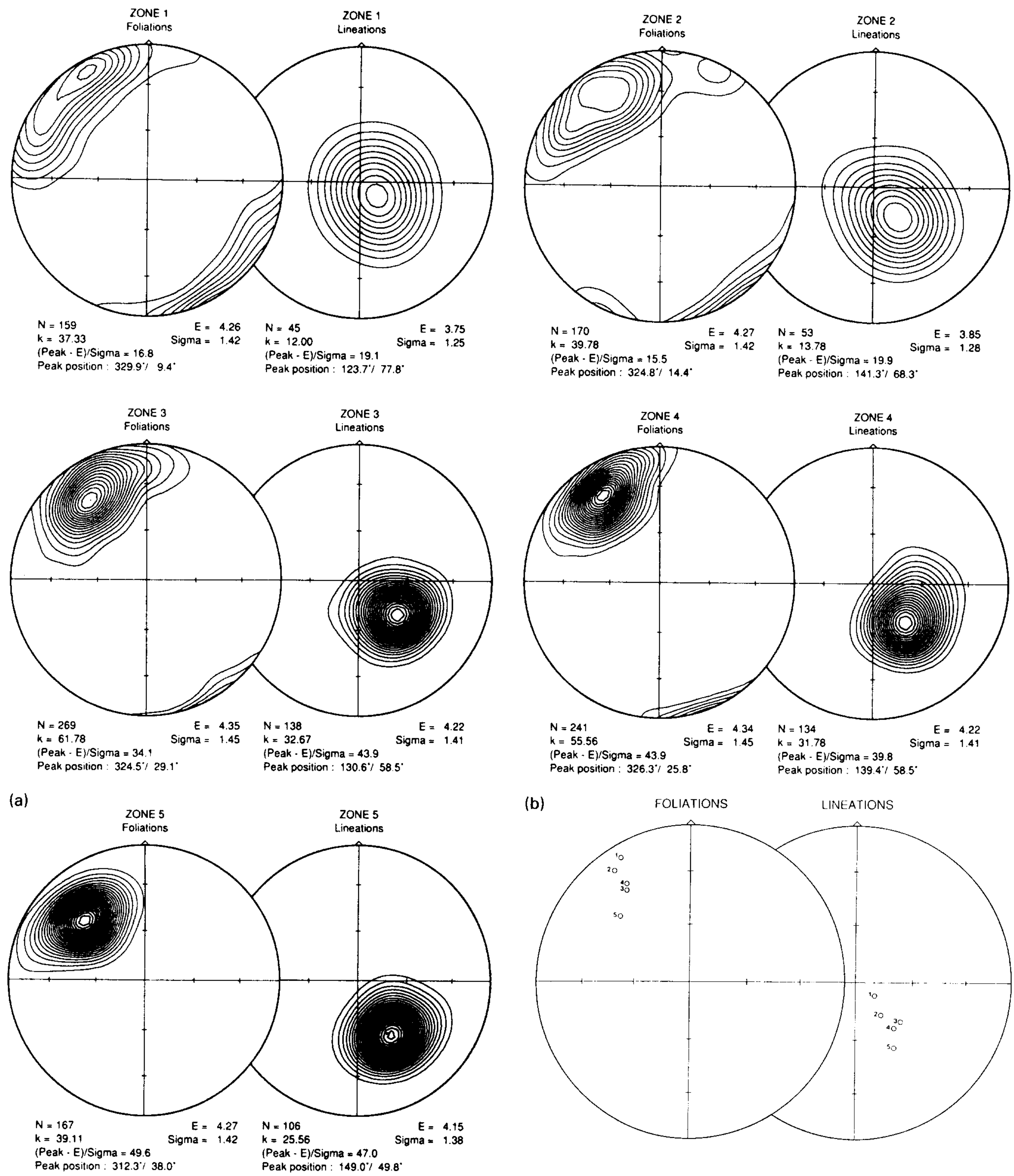

Fig. 2. Structural element data for the five mesostructural zones described in the text. (a) Shown in order from northwest to southeast on lower-hemisphere projections are lineations and poles to foliations. The lowest contour in each plot represents an even distribution (E), the value for which is determined by the number of data points (N) in each plot (Robin & Jowett 1986). Peak values are given in standard deviations (σ) above E. The contour interval is 2σ. (Plotting program, Frontenac Wordsmiths, 1990.) (b) Compilation fabric diagrams which include all data shown in (a). The change in dip of the foliations and the decreasing plunge of the lineations is apparent. Also note the orientation of the lineations along the true dip of the foliations. Numbers refer to mesostructural zones in Fig. 1.

The oldest pegmatites are invariably mylonitized and trend parallel to the main fabric in the host rock. Younger dykes are gently to isoclinally folded with foliation-parallel axial surfaces or, rarely, undeformed.

Zone 3 is a single, broad deformation zone chararacterized by a lithologically banded series of ultramylonites that follow the southeast boundary of the Bell Lake Granite. In general the boundaries of zone 3 coincide with the boundaries of the JLSZ. The mylonite on the southeast boundary of the JLSZ is fine-grained but not

Table 1. Summary of fabric data

	Foliations			Lineations		
Zone	Strike (°)	Dip (°)	Peak*	Azimuth (°)	Plunge (°)	Peak*
1	59.9	80.6	16.8	123.7	77.8	19.1
2	54.8	75.6	15.5	141.3	68.3	19.9
3	54.5	60.9	34.1	130.6	58.5	43.9
4	56.3	64.2	43.9	139.4	58.5	39.8
5	42.3	52.0	49.6	149.0	49.8	47.0

*(Peak count − E)/σ.

glassy and displays a well-developed *S–C* texture. Ultramylonites on the northwest boundary are generally glassy.

Zone 2 is underlain by non-foliated to foliated units of the Killarney complex and contains the main body of the Bell Lake Granite. These units are locally cut by thin, discontinuous zones of mylonite. The intensity of the fabric developed decreases toward the northwest as does the frequency of minor shear zones. The rocks in these shear zones range texturally from ultramylonite with a micrometer scale grain-size to cataclasite.

Zone 1 is underlain by the contact between the mid-Proterozoic intrusives of the Killarney complex and the Huronian metasediments. Deformation in this zone is generally characterized by cataclasis, with brecciated blocks surrounded by either a matrix of fine cataclasite (Fig. 4a) or vein quartz. Rarely, thin seams of pseudotachylyte occur. Regionally this zone follows the same trend as the GFTZ; individual fractures and faults, however, exhibit no preferred orientation (O'Donnell 1986).

Samples of granitic rock with different amounts of strain have been collected across these five zones and thin sections examined to characterize the nature of the

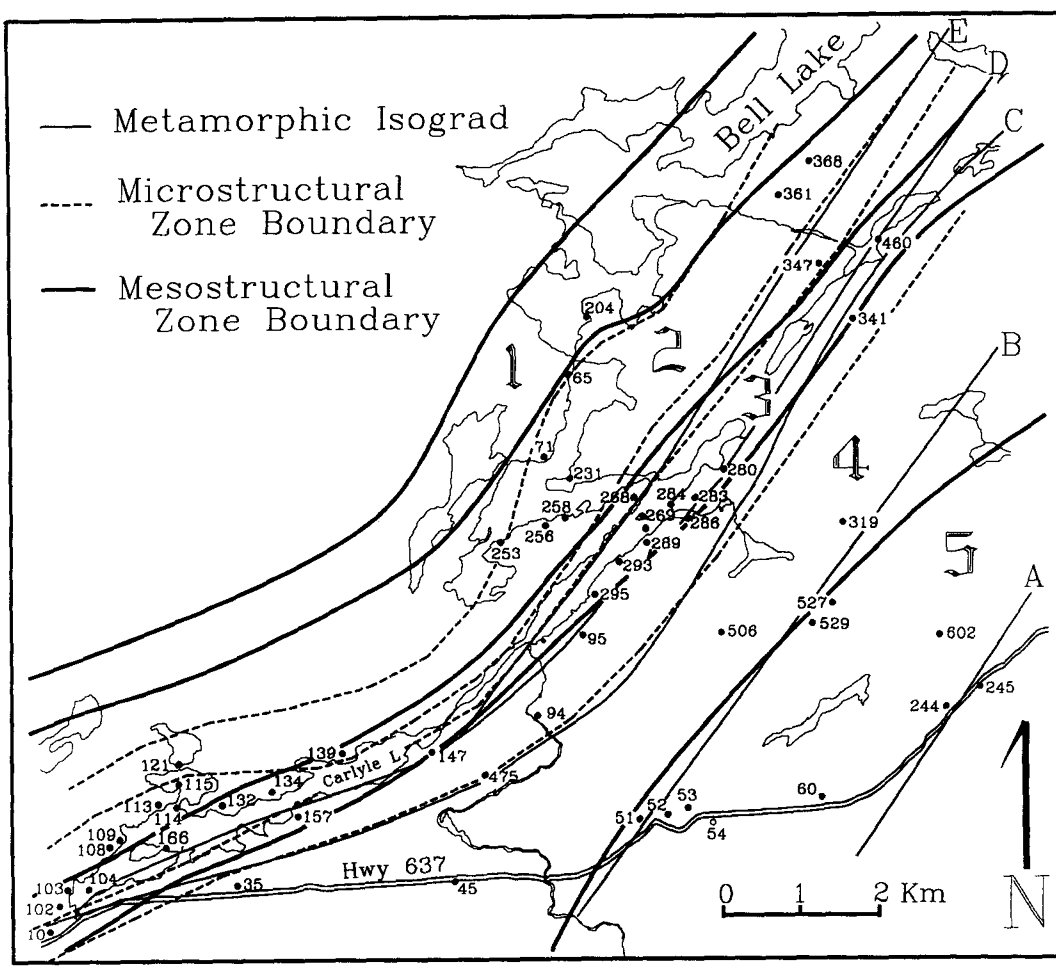

Fig. 3. Isograds (light solid lines), microstructural divisions (dashed lines) and mesostructural divisions (heavy solid lines). Isograds are based on the appearance or disappearance of minerals across the area: A—biotite in; B—muscovite in; C—albite + epidote in, hornblende out; D—chlorite in; E—garnet and sillimanite out. Microstructural boundaries are based on the change in the predominance of one type of microstructure for another as described in the text and Fig. 5. Sample locations indicated as numeric only.

deformation in feldspar during mylonite formation at various metamorphic grades. Both mylonitized and relatively undeformed samples from each zone were examined in order to distinguish which features were specifically related to mylonite formation. All thin sections were cut parallel to the stretching-lineation and perpendicular to the foliation (i.e. the *XZ* plane of the finite strain ellipsoid) and stained for K-feldspar identification. Polished sections examined on the microprobe give K-feldspar compositions of Or_{85-97} (the %Or increasing from southeast to northwest), and plagioclase compositions of An_{14-24} for samples from the southeastern half of the area and An_{1-24} for samples from the northwest. The locations of all samples to which reference is made are shown on Fig. 3.

A kinematic analysis based on fabric asymmetry, tails on feldspar augen, mica-fish (Lister & Snoke 1984) and quartz microstructures (Boullier & Bouchez 1978) has been carried out to deduce the sense of movement on the *C*-surfaces. Kinematics in this area are extremely consistent and indicate a southeast-side-up sense of displacement on steeply- to moderately-dipping *C*-surfaces that possess a well-developed down-dip stretching lineation (Pryer 1985).

Metamorphism

This study has been confined to the granitic (*s.l.*) units occurring in the map area. Table 2 gives the mineral assemblages stable during deformation for each thin section studied. Criteria used to determine mineral stability during deformation include: presence in *S*- or *C*-surfaces, presence within grain-scale microfaults, presence within feldspar pull-aparts, and new grains produced through dynamic recrystallization at grain boundaries.

Although these rocks contain minerals that are relatively stable over large portions of *P–T*-space, a general and continuous decrease in metamorphic grade from amphibolite to greenschist can be recognized from southeast to northwest. Simplified mineral isograds are shown in Fig. 3 broadly based on (A) the appearance of biotite, (B) the appearance of muscovite, (C) the

Table 2. Mineral assemblages

Sample	Chlorite	Epidote group	Muscovite	Biotite	Garnet	Sillimanite	Hornblende	Albite	Oligoclase
P204	x	x	x	x					
P65	x	x	x	x				x	
P121	x	x	x	x					
P256	x	x	x	x					
P115		x	x	x					
P113		x		x					
P114	x	x	x						
P109		x	x	x				x	
P108	x	x	x	x					
P368		x	x	x					
P361		x	x	x					
P132		x	x	x					
P134	x	x							
P139	x	x	x	x				x	
P104		x	x	x					
P102		x	x	x					
P147	x	x	x						
P157		x		x				x	
P347		x	x	x	x	x			
P268		x	x	x	x				
P269		x	x	x	x	x			x
P283	x	x		x					
P280	x	x							
P286	x				x				
P460	x	x	x	x	x				
R95		x	x	x	x				
P94		x		x					
P10			x		x		x		x
P475		x		x			x		
P35				x	x		x		
P506				x	x				
P529		x		x			x		
P527		x		x					
P45			x	x		x			
P51			x	x		x			
P52				x					
P53				x					
P54				x					
P60				x					
P244				x	x	x	x		x
P245					x		x		

All assemblages include quartz + K-feldspar + plagioclase.
Plagioclase compositions determined by microprobe analysis only for those indicated.

appearance of albite + epidote and the disappearance of blue-green hornblende, (D) the appearance of chlorite and (E) the disappearance of garnet and sillimanite. In general, the isograds are sub-parallel to the meso- and microstructural boundaries (heavy solid and dashed lines, respectively, on Fig. 3), but isograds and mesostructural boundaries tend to diverge toward the northeast. The position of the isograds northward from the JLSZ indicates that the metamorphic grade, the availability of water (Passchier 1985), or both, increases along the Grenville Front in the JLSZ northeastward. The similar divergence of microstructural boundaries and isograds relative to the mesostructural boundaries illustrates the dependence of strain-induced deformation and recovery features which track changes in the same manner as mineralogy. There is therefore potential for the use of microstructures as indicators of metamorphic grade during deformation.

Quartz microstructures indicate that dynamic recrystallization was operating in quartz in all zones other than zone 1. The thermal activation of intracrystalline creep in quartz and therefore the lower limit of dynamic recrystallization occurs in wet quartz between 250 and 300°C (Tullis 1978). Assuming a linear geothermal gradient of 20°C km^{-1} (White & White 1983), this would occur at a depth of 15 km. Ternary-feldspar-geothermometry (Fuhrman & Lindsley 1988) gives an equilibrium temperature for a sample from southeast zone 5 (P244; Fig. 3) in amphibolite grade at 530°C ± 40°C, corresponding to a depth of 25–30 km. This is a minimum temperature due to the ability of feldspar to re-equilibrate at high temperatures, especially during deformation (Yund & Tullis 1991). There has therefore been a differential vertical displacement from southeast to northwest of more than 10 km.

VARIATIONS IN FELDSPAR MICROSTRUCTURES

The variation in microstructures observed in the five mesostructural zones (Fig. 1) are described below and summarized in Fig. 9. Examination of microstructures has resulted in the microstructural boundaries shown in Fig. 3. The mesostructural and microstructural zone boundaries are sub-parallel, but the microscopic style of deformation is much less dependent on lithology or the existence of lithological contacts.

Zone 5

In the southwestern corner of zone 5 mylonite is rare. Quartz occurs in ribbons of elongate rectangular grains (Type 4 quartz ribbons; Boullier & Bouchez 1978) or as large polygonized grains in pressure shadows at the ends of feldspar grains (Fig. 4b). Elongate feldspar grains define the gneissic foliation and control the quartz ribbon orientation. Feldspar–quartz grain contacts are very smooth and straight. Both plagioclase and K-feldspar in contact with other feldspar or hornblende grains generally display a core-and-mantle texture (White 1975). (A core and mantle texture is used here as a purely descriptive term for any feldspar grain with a more deformed outer zone or mantle and a much less deformed inner zone or core.) Feldspars with highly serrated grain boundaries are surrounded by a mantle of fine recrystallized grains. Recrystallized grains are either the same composition as the core, i.e. oligoclase or Or_{84-88} in both core and mantle, or a different composition, i.e. Or_{84-88} core with a mantle containing both plagioclase and K-feldspar grains. Dynamic-recrystallization also occurs on the boundaries of hornblende grains. Some feldspar mantles are composed of subgrains of varying misorientation but are generally no more than two subgrain diameters wide. Generally optical subgrain-size is twice the matrix or recrystallized grain size. Feldspar cores display undulatory extinction and show some fracturing. These fractures show no offset and display a variety of distributions (P52, P54, P244 and P602; Fig. 10).

Twins are extremely rare in plagioclase grains, and K-feldspar displays polysynthetic twinning only in very small patches around tiny cracks within the grain, on impingement-point contacts on grain boundaries or locally along the boundaries of inclusions. Rarely, small matrix K-feldspar grains are completely twinned. Some K-feldspar grains are microperthitic with plate, bead or braid textures (Smith 1974). Myrmekite is common on K-feldspar grain boundaries that are parallel to the *S*-foliation (Fig. 5a).

Zone 4

In *S–C* mylonites (mode I *S–C* mylonite of Lister & Snoke 1984), oligoclase grains vary from equant to slightly inequant and are generally subrounded in outline. The long diameters of inequant grains are sub-parallel to the quartz ribbon elongation direction. The boundaries of the large plagioclase grains are serrated where they meet other feldspar grains but otherwise are smooth. Very small feldspar grains are found along the serrated grain boundaries.

In oligoclase, twins are very thin and taper to a point or end abruptly within a grain and are commonly bent. All twins appear to be mechanically produced, identified on the basis of morphology (Smith 1974, Jensen & Starkey 1985, Smith & Brown 1988). Kink bands occur with narrow diffuse boundaries and traverse entire grains (Fig. 6a). The kink bands invariably occur at an angle of 25–30° to the *C*-foliation direction and are invariably oriented at a high angle (sub-normal) to the twin lamellae which can be seen to bend into and out of the bands. The twin lamellae are oriented approximately 60° to the *C*-foliation and 15–30° to the *S*-foliation direction.

Polysynthetic twins occur in some matrix K-feldspar grains and are irregularly distributed in larger grains similar to that described for zone 5. Intracrystalline microkinking (Fig. 6b) is observed only rarely and is restricted to K-feldspar. Where present, however, a large number of microkinks occur within a single K-

4.

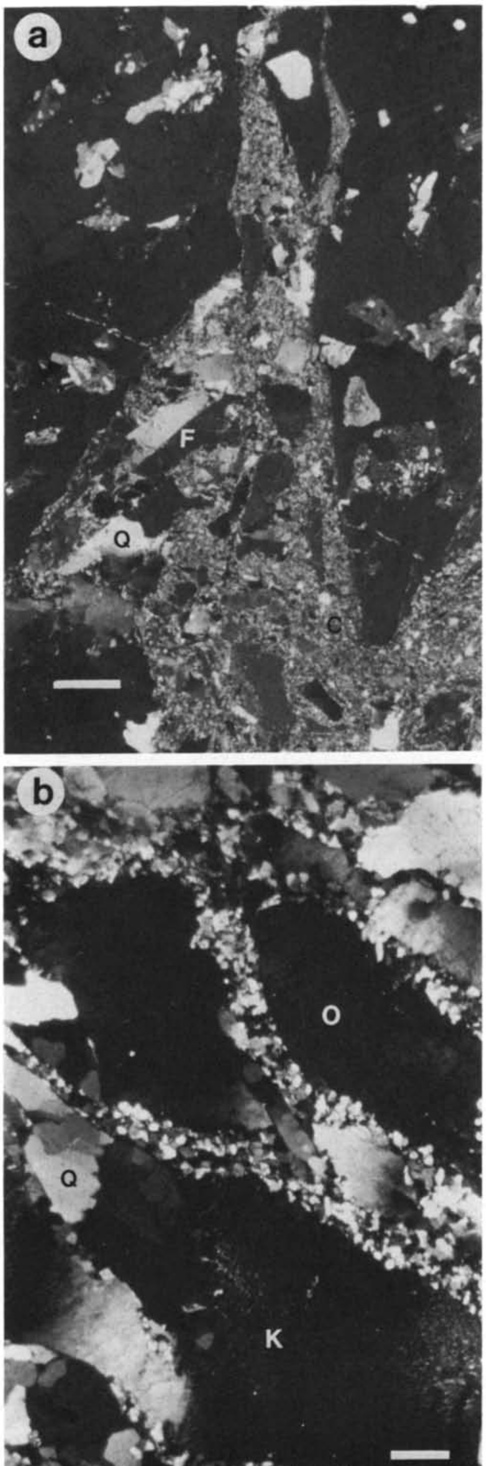

5.

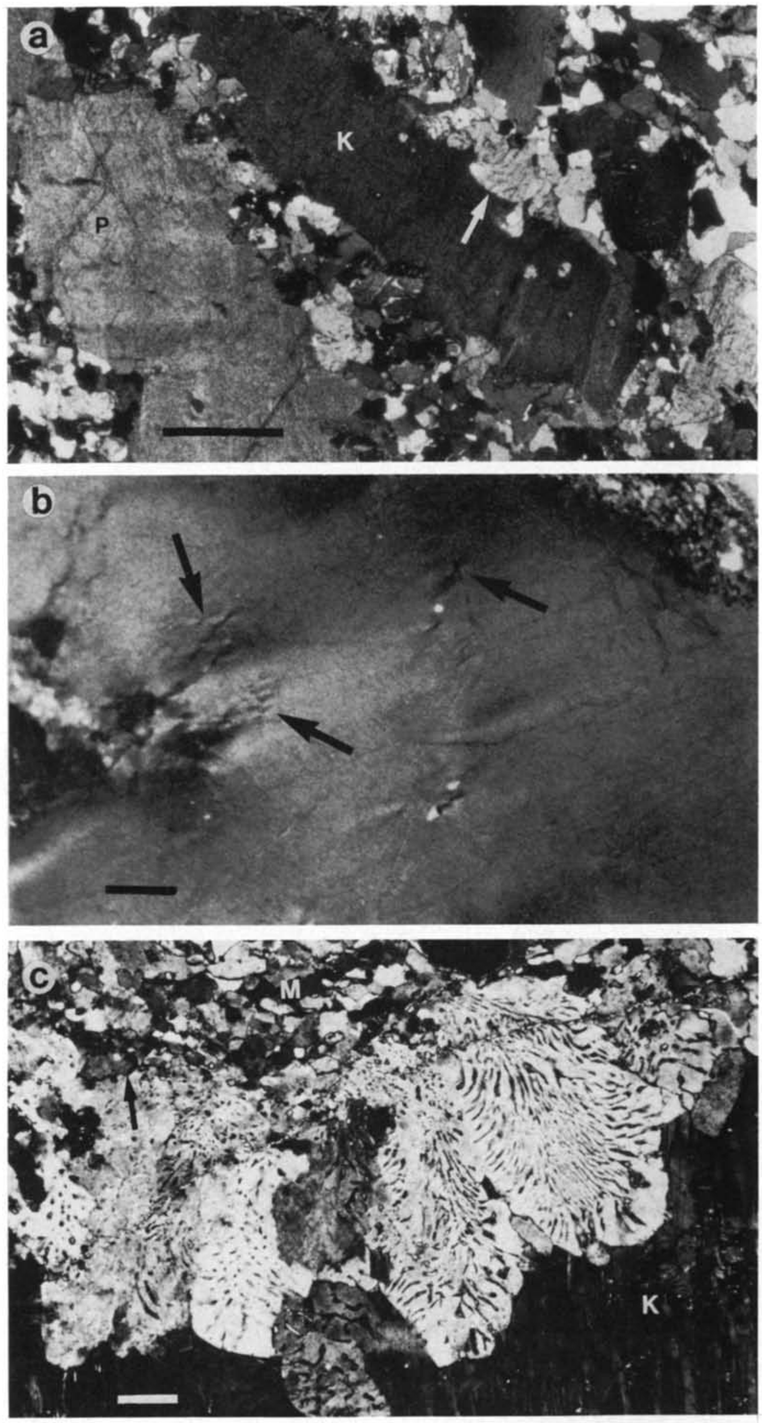

Fig. 4. (a) Fault gouge in microfault within the Bell Lake Granite. The fault gouge consists of angular fragments of quartz (Q) and feldspar (F) in a fine cataclasite matrix. Scale bar is 0.5 mm. P204. (b) Texture of augen gneiss from zone 5. Large, inequant feldspar grains, both oligoclase (O) and microperthitic K-feldspar (K), which control the quartz ribbon orientation and define the foliation, are surrounded by recrystallized mantle grains. Hornblende from this sample also displays a core-and-mantle structure. Note the large quartz-subgrain-size (Q). Scale bar is 0.5 mm. P244.

Fig. 5. (a) Myrmekite (arrow) on the boundaries of a K-feldspar grain from zone 5. K—K-feldspar; P—Plagioclase. The long axes of the feldspars define the *S*-foliation in this sample. Scale bar is 0.5 mm. P529. (b) Intracrystalline microkinking (arrows) in K-feldspar from the southeast-side of zone 3. Scale bar is 0.1 mm. P10. (c) Well-developed myrmekite (centre) on a K-feldspar grain boundary from the southeast-side of zone 3. K—K-feldspar (bottom); M—matrix (top left). Note the highly serrated interface (arrow) between the myrmekite and the matrix. Scale bar is 0.1 mm. P10.

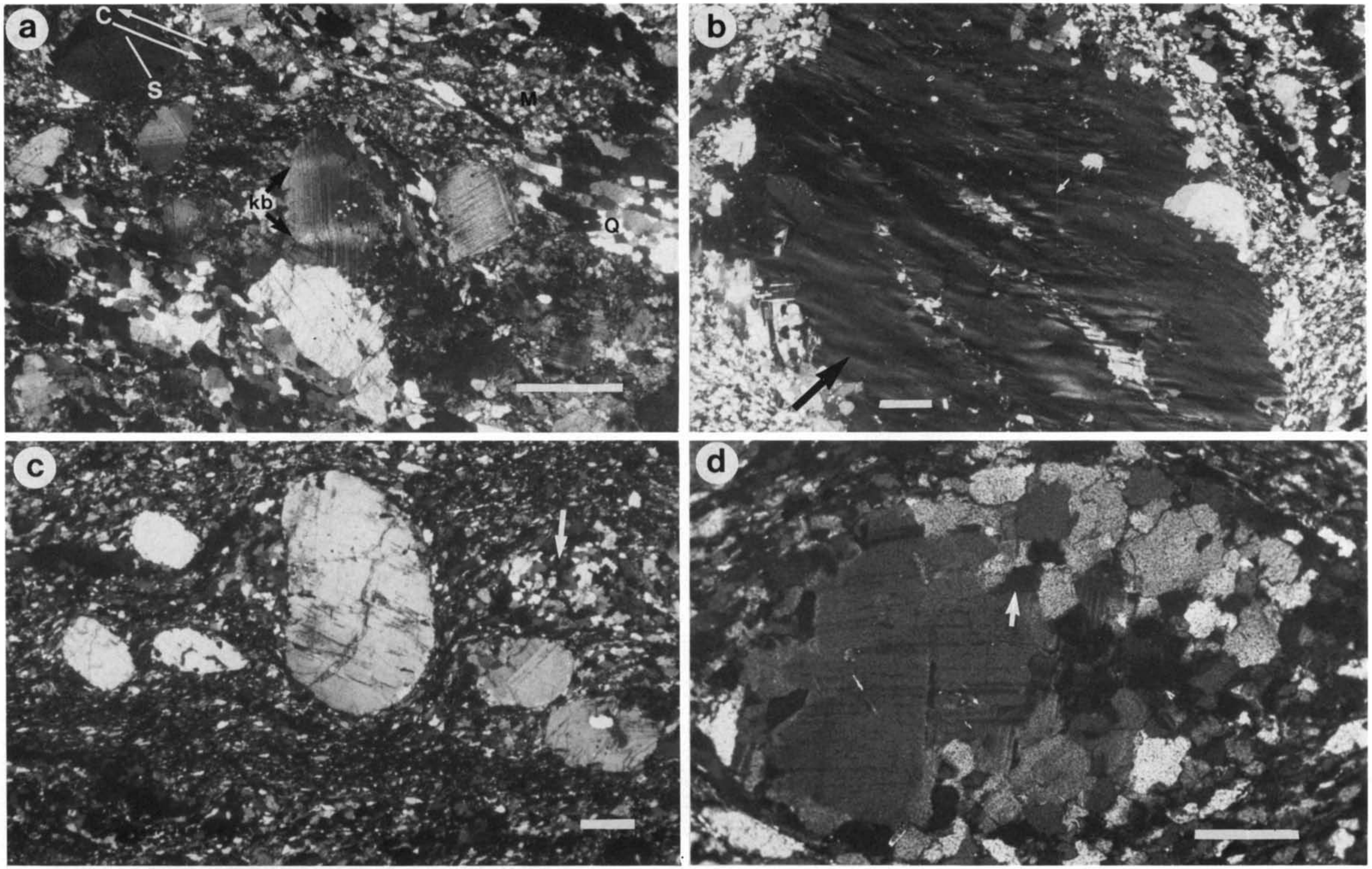

Fig. 6. Microstructures from zone 4. Scale bars are 0.5 mm. (a) Plagioclase with deformation-twins and two kink-bands (kb) with diffuse boundaries. Note the large grain size in the quartz ribbons (Q) relative to the finer grain size of the feldspar matrix (M). The orientation of *S*- and *C*-surfaces, as well as the sense of displacement on the *C*-surface, are indicated. P35. (b) Internal deformation of an orthoclase grain-core which contains elongate zones of plagioclase (note twinning) and displays an abundance of microkinks (e.g. large arrow) which probably developed as a result of pinned dislocations. Shear fractures which trend at a high angle to the albite zones (e.g. small arrow) appear to offset the undulations. The grain-boundary shows evidence of recrystallization by its serrated appearance. Recrystallized grains at the perimeter of the orthoclase are dominantly composed of albite. P35. (c) Well-rounded oligoclase porphyroclasts from an augen ultramylonite of granodioritic composition. Note the varying orientation of long axes from one grain to the next. Coarser-grained area (arrow) is probably the remnant of a completely recrystallized grain. P35a. (d) Dynamic recrystallization by subgrain rotation in oligoclase (e.g. arrow). Recrystallized grain-size generally decreases toward the outer mantle where the mantle is indistinguishable from the matrix. P35a.

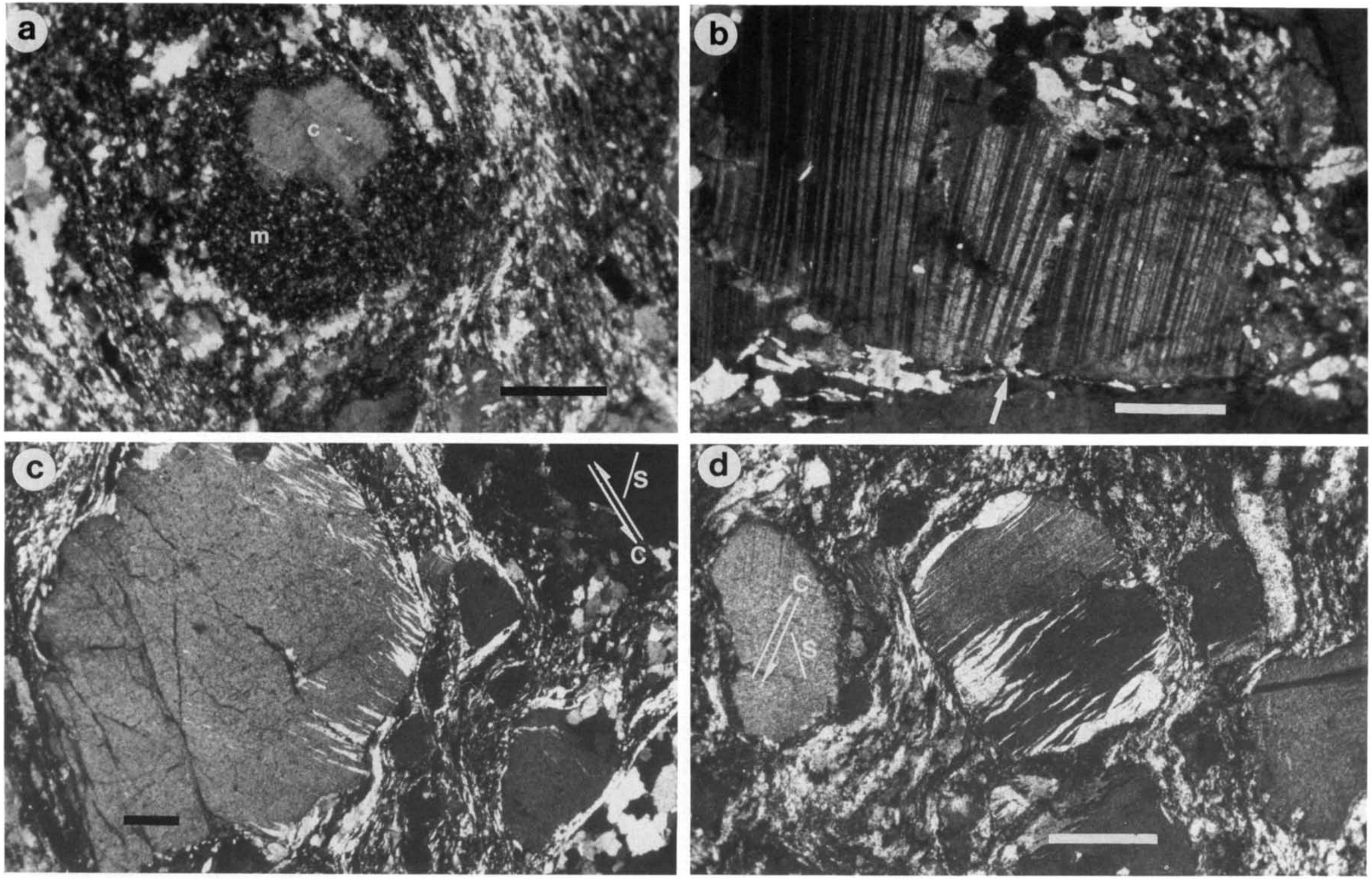

Fig. 7. Internal deformation features from feldspars of zone 3. Scale bars are 0.25 mm. (a) Well developed core (c) and mantle (m) structure in a K-feldspar within an augen ultramylonite as a result of neocrystallization. Hydrous alteration is apparent in plagioclase from the same sample. P460. (b) Recrystallization in plagioclase similar to Type-2 segregation bands described by Hanmer (1982). Grain misorientation across the band (arrow) is indicated by the misorientation in twin lamellae. P10. (c) Perthite flames in a K-feldspar augen. Flames trend approximately normal to the foliation. The grain has been fractured internally. P347. (d) Flame perthite in a well-rounded K-feldspar porphyroclast. A slight difference in orientation between the upper and lower halves of the grain (indicated by the difference in grey level) may be responsible for the difference in the extent of flame development. Flame orientation is normal to the main trend of the foliation (as indicated) in this sample. Note albite at grain ends in pressure shadow locations. P139.

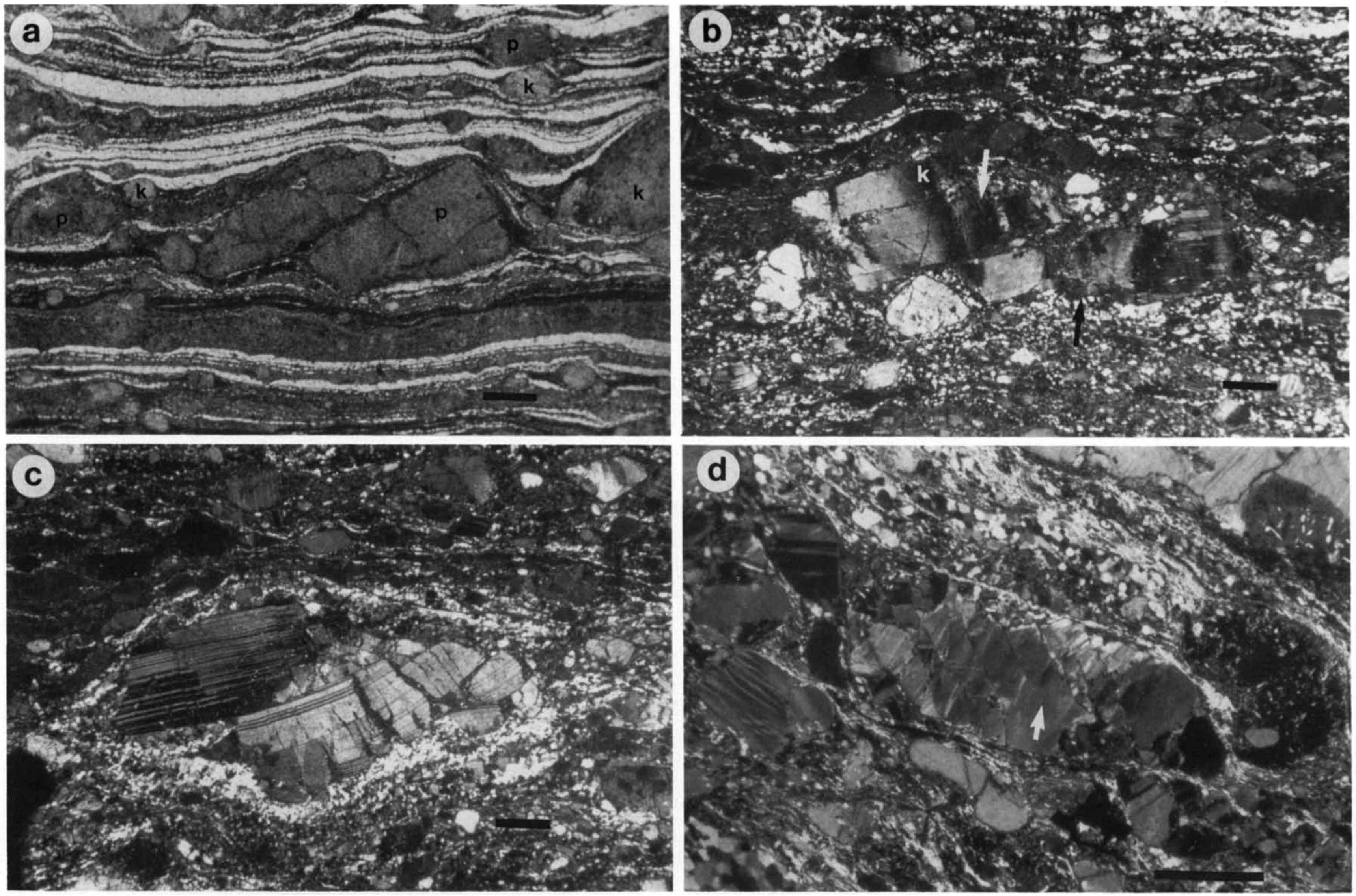

Fig. 8. Grain scale faults in feldspars. Shear sense on the well-defined (*C*) foliation in all cases is sinistral. Scale bars are 0.5 mm. (a) Fracturing and separation of both plagioclase (p, dark grey) and K-feldspar (k, light grey) along the foliation in an uiltramylonite from zone 3. Individual strings of connected augen are restricted to a single feldspar composition. Plane light; sample has been stained for both K- and Ca-feldspar identification. P269. (b) Plagioclase grain from zone 3. Synthetic shear fractures have displaced fragments. Each fragment contains kink bands (k) and microkinks (zone of irregular extinction, white arrow) as well as a cataclastic zone (black arrow) all of which appear to pre-date the shear fracture. Complete separation of these fragments will produce feldspar 'fish' (Mawer 1987). P102. (c) Two fracture types in plagioclase. Synthetic shear fracture (sinistral) occurs at a low angle to the foliation and is parallel to both the cleavage and the twinning in the crystal. Antithetic fractures (dextral) are coarse and irregular and cut cleavage and twins at a high angle. All fragments of the grain contain abundant deformation twins produced at various times relative to the development of the fractures. The synthetic fracture both cuts and is cut by antithetic fractures. Overall sinistral sense-of-shear is indicated by the fabric asymmetry in the matrix. (d) Antithetic fractures in plagioclase from zone 2. The overall shear sense in the specimen is sinistral. The sense of offset across each fracture is dextral. Individual fragments have rotated in a counter-clockwise direction. Arrow shows termination of an incomplete fracture. P231.

feldspar grain. Myrmekite is found along K-feldspar grain boundaries that are parallel to the *S*-foliation direction (e.g. see Simpson 1985, Simpson & Wintsch 1989). Undulatory extinction is ubiquitous in large grains of plagioclase and K-feldspar.

Fracturing in feldspars is common, but the fractures are generally short and discontinuous. Fractures occur at the boundary or isolated within a crystal. Approximately one-half of the fractures observed occur along crystal cleavage planes. Fracture orientation distribution is either isotropic (e.g. P10 and P35, Fig. 10) or extremely anisotropic with the maximum oriented 60–70° from *C*, subparallel to *S* (e.g. R95, P527 and P529, Fig. 10). These fractures show no displacement. Some fractures contain quartz, biotite and/or epidote.

In ultramylonite, feldspars occur as porphyroclasts widely dispersed throughout a fine-grained foliated matrix of quartz and feldspar. The majority of porphyroclasts are oligoclase; K-feldsar porphyroclasts are rare but some very large ones (>1 cm) do occur. Porphyroclasts vary from largely equant to inequant. The long axes of inequant grains have variable orientations relative to the mylonitic foliation (Fig. 6c) (cf. Ghosh & Ramberg 1976). Many porphyroclasts have smooth outlines, i.e. with no obvious mantle, although the boundaries are serrated. Others have a well-developed mantle of subgrains. The misorientation of subgrains within cores increases into the mantle (Fig. 6d). Grain-size within the mantle is variable but generally decreases toward the outer mantle. The fine-grained outer mantle is impossible to differentiate from the matrix. The well-rounded porphyroclasts, as well as the cores of many mantled augen, show very little evidence of internal deformation other than minor fracturing.

Zone 3

While zone 3 is essentially a single wide shear zone, the adundance and type of microstructures present change systematically from southeast to northwest in conjunction with a decrease in the metamorphic grade. On the southeast side of zone 3 (i.e. the southeast side of the JLSZ), the deformation of feldspars is dominantly intracrystalline, with fracturing only of minor importance. The most common feature observed is recrystallized grains at grain boundaries, producing a core-and-mantle structure. The recrystallized grain-size is equivalent to the matrix grain-size and shows little variation within a sample. The core feldspar grains are generally 1–2 orders of magnitude larger than the mantle and matrix grains. The widths of recrystallized mantles are very small relative to core diameters, and cores have highly serrated boundaries. In some samples, mantle grains are the same composition as the core grain they surround while in other samples both K-feldspar and oligoclase cores are mantled with albite (Fig. 7a). Recrystallization also occurred in narrow straight bands that cross grain cores. There is measurable lattice misorientation across these bands (Fig. 7b), seen either as abrupt changes in extinction or as slight changes in orientation of twin lamellae. These recrystallized bands resemble Type-2 segregation bands of Hanmer (1982).

Undulatory extinction in both plagioclase and K-feldspar is irregular due to intracrystalline microkinking and microfracturing. In K-feldspar, microkinks are very small and usually occur close to the grain boundary (Fig. 5b). In plagioclase, entire grains show sharp kinked, extinction patterns like the reflections from crinkled aluminium foil. Deformation twins and kink-bands are also present in plagioclase. Myrmekite is ubiquitous in K-feldspar grains (Fig. 5c), most notably on the long sides of inequant grains which invariably face the finite shortening direction. Fracturing of grains is rare; those fractures which do occur are minute and show no offset.

Flame perthite occurs in zone 3 and consists of flames of albite in a K-feldspar host. Flames originate at grain boundaries or along internal grain fractures, the majority of which are oriented sub-parallel to the flattening foliation (Fig. 7c). The flames themselves trend perpendicular to those boundaries and are therefore normal to the flattening (*S*) plane. Flames may also radiate away from a point contact between adjacent feldspar grains, i.e. at stress concentration points, or develop in typical pressure shadow positions (Fig. 7d). Flames are generally widest at the grain boundary and taper to a point within the grain.

Along the northern boundary of the mylonites in zone 3 (JLSZ), feldspars show grain-size reduction through continued fracturing and separation of broken fragments along the shear foliation (mylonitic foliation; Fig. 8a). Fractured fragments still in contact with one another are angular. Isolated feldspar fragments are rounded. The sense of displacement on grain-scale faults is typically synthetic to the offset sense on the *C*-surfaces (Figs. 8a & b and 10). A wide range of grain-sizes (0.005–10 mm) is present in all samples. Generally, grains with diameters larger than 0.7 or 0.8 mm are fractured, usually along cleavage planes, into rectangular fragments. Smaller grains are rounded and display very little fracturing. Strings of feldspar augen are commonly connected along the foliation by a thin band of very fine-grained (8 μm) feldspar (Fig. 8a). Individual strings are generally restricted to a single feldspar composition (i.e. either plagioclase *or* K-feldspar, evident after staining for both Ca and K) and are separated from one another by parallel bands of very fine-grained quartz (Type 2 quartz ribbons; Boullier & Bouchez 1978). Deformation bands, kink bands (Fig. 8b) and mechanical twins are ubiquitous in this zone. Flame perthite is commonly developed to such an extent that the grains may be composed of half albite and half K-feldspar.

Zone 2

Microstructures indicating crystal-plastic deformation decrease in abundance both to the northwest, normal to the mesostructural boundaries, and to the southwest, parallel to the GFTZ, and ultimately disappear. Mechanical or glide twins are ubiquitous throughout this zone. Glide twins, which occur in locally hydrated

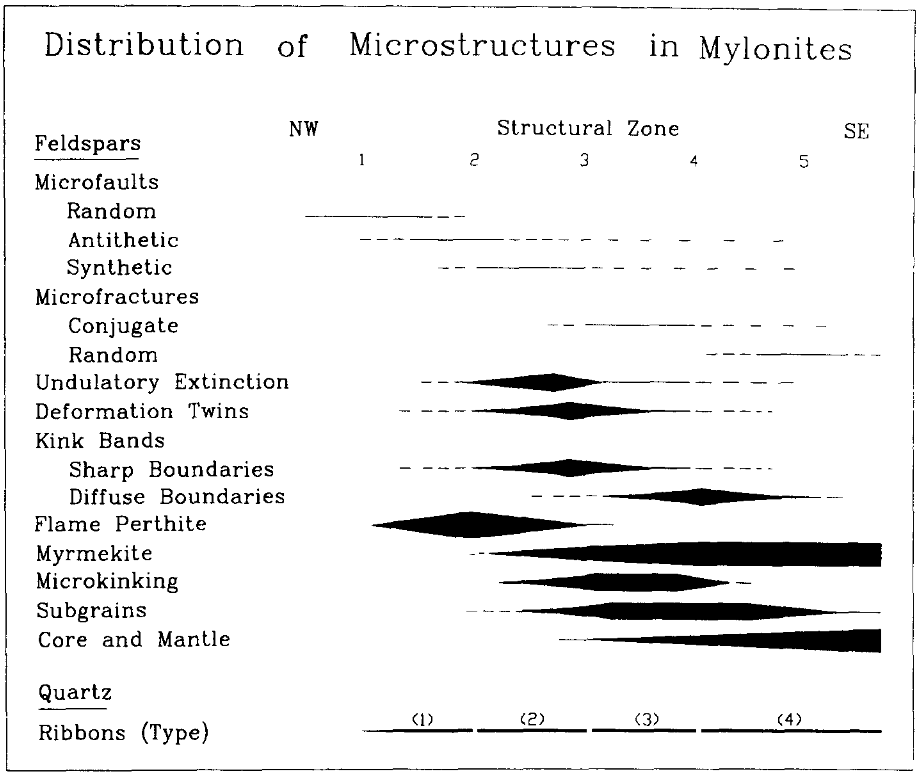

Fig. 9. Range diagram for microstructures described in the text. The width of the line indicates the relative importance of each feature as a textural element in each area. (Quartz ribbon type refers to those defined by Boullier & Bouchez 1978.)

plagioclase, are offset across grain-scale faults. Twins often bend near faults, or occur only on one side (Fig. 8c). Individual twins often vary in thickness along their length, most dramatically in bent crystals. Undulatory extinction, deformation bands and kink-bands are common in plagioclase. In K-feldspar, polysynthetic twins are irregularly distributed. Flame perthite is common and, rarely, myrmekite occurs along the S-parallel grain boundaries in K-feldspar grains such that both features may occur along a single grain boundary.

The dominant microstructures in the feldspars of zone 2 are discrete grain-scale faults that occur singly or in conjugate sets (Fig. 8c). As in the northwest portion of zone 3, there is a wide range in grain size. Approximately 50% of fractures and faults in grains with diameters of 0.5 mm or larger utilize the feldspar cleavage. The utilization of a crystal cleavage by a fracture may change from one fracture to the next within a grain or it may change along the length of a single fracture. Antithetic grain-scale faults (with a sense of offset opposite from the deduced sense of movement on the shear (C) foliation) are more than twice as frequent (fracture frequency diagrams summarized in Fig. 10) as synthetic faults. Antithetic faults are generally filled with fine-grained quartz, feldspar or phyllosilicates. Many feldspar grains are broken down into angular fragments. Some fractures do not cut the grains completely. Displacement along these fractures produces feldspar 'dominoes' (Tullis 1978) (Fig. 8d). Grains smaller than 0.5 mm are generally subrounded in outline with few optically visible internal fractures.

Zone 1

The feldspars in zone 1 have undergone deformation by fracturing and brecciation. Fractures within grains are randomly oriented and are variously filled with mica, epidote or gouge. Randomly oriented microfaults that transect many gains are common. They contain angular and brecciated fragments of both quartz and feldspar in a very fine cataclasite matrix (Fig. 4a).

DISCUSSION

Recovery features

The fabric on the southeastern side of zone 5 is indicative of high-temperature creep in all mineral species. The penetrative and symmetric fabric and lack of localized mylonites indicates that these rocks were capable of ductile flow with no tendency for shear localization at the scale of the outcrop or hand specimen. The rock fabric in the remainder of zone 5 and zone 4 is strongly asymmetric. An S–C fabric is present throughout and localized bands of ultramylonite are common. Evidence for recovery in feldspars is abundant throughout zones 4 and 5. The temperature at which this deformation took place must have been at or above $0.5T_m$ of feldspar (and hornblende in southeast zone 5), the temperature required for recovery. Recovery processes include both subgrain rotation and dynamic recrystallization through grain-boundary migration. In K-

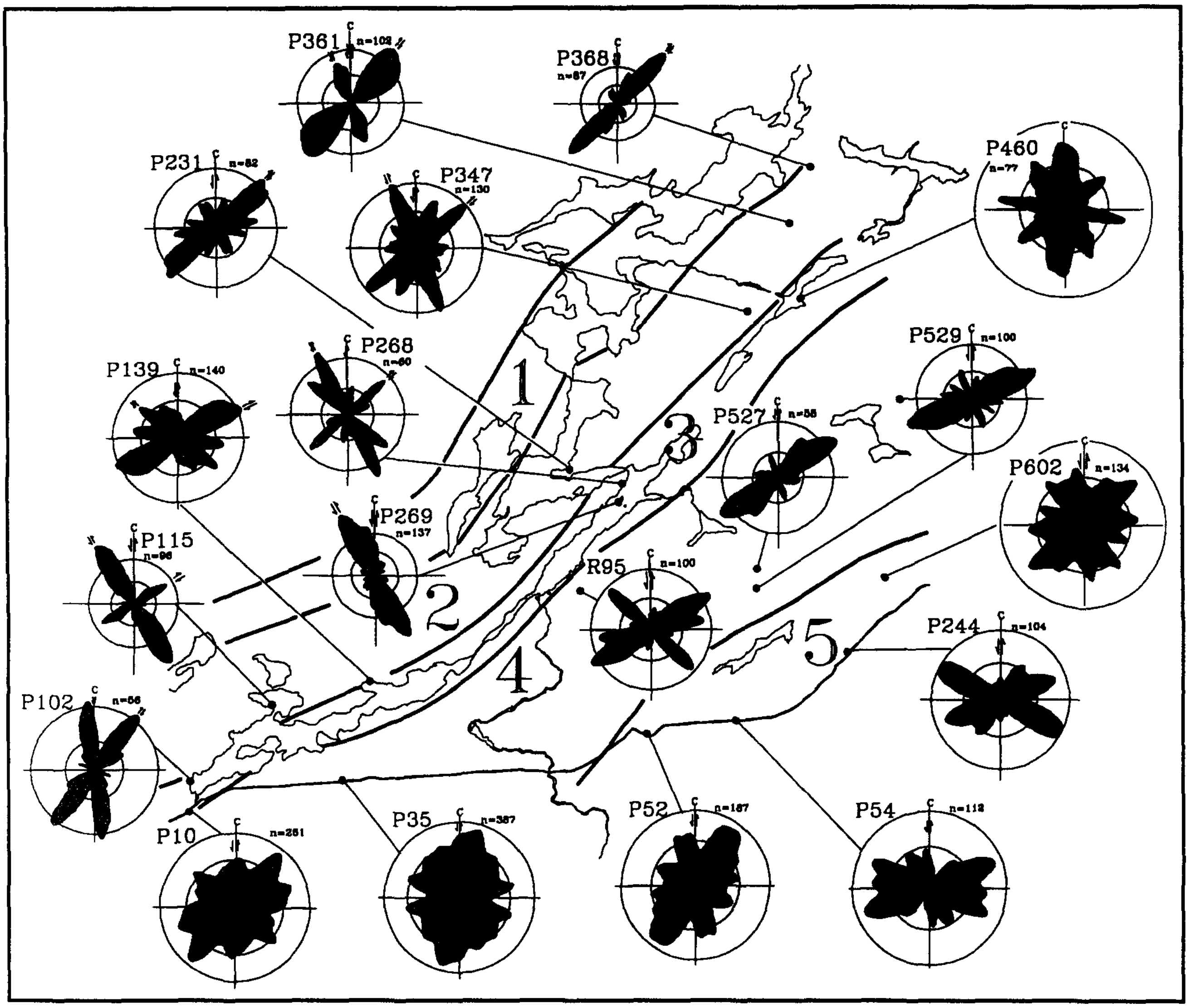

Fig. 10. Rose diagrams of feldspar fracture orientations from the map area. Section measured in each case is subvertical in orientation with northwest to the left, southeast to the right. Fractures were measured relative to the foliation which occupies a vertical position. Antithetic fractures are dextral and occur in the northeast quadrant; synthetic fractures are sinistral and occur in the northwest quadrant. The largest diameter circle represents the position of 1.8σ above an even distribution. The circle with the next smallest diameter represents the value for E. In those plots with three circles, the smallest circle represents $E - 1.8\sigma$.

feldspar, grain-boundary migration has resulted in some recrystallized grains of a totally different composition (cf. Yund & Tullis 1991). The different recovery mechanisms indicated by these microstructures are interpreted to be due to local variations in stress distribution and strain-rate. Similar microstructures have been observed in feldspars by others (e.g. Olsen & Kohlstedt 1980, Vidal *et al.* 1980) in rocks deformed naturally at temperatures greater than 550°C.

In the *S–C* mylonites, the boundaries between adjacent feldspar grains are highly serrated, indicating dynamic recrystallization through grain-boundary migration. Serrated boundaries are not developed however between feldspar and biotite or quartz. This illustrates the strain localizing ability of feldspar (Tullis & Yund 1980). Dynamic recrystallization occurs by subgrain rotation in ultramylonite (Fig. 6d) as well as by grain-boundary migration, indicating that both climb-accommodated and recrystallization-accommodated dislocation-creep were operating in the same sample. The general lack of internal deformation in the augen in ultramylonites suggests that, as the proportion of matrix that can accommodate a much higher strain-rate increases (e.g. Fig. 6c), the velocity field in the ultramylonite becomes more heterogeneous and accounts for the difference in deformation mechanisms indicated by some feldspar augen. There appears to be no compositional control on the type of recovery here, i.e. climb vs recrystallization, so the augen with mantles consisting of subgrains are interpreted to have undergone deformation at a lower strain-rate than those with dynamically recrystallized mantles. The similarity in grain-size between the dynamically-recrystallized grains and the matrix grains indicates that it is these grains that are most stable. In mantles produced by subgrain rotation, the decrease in grain-size from inner to outer mantle can be accounted for by an increase in strain-rate away from the grain core such that the subgrains in the outer mantle may undergo recrystallization-accommodated dislocation-creep. The main conclusion that can be drawn from these observations is that the natural strain-rate, at least for these mylonites, was too high to allow recovery by climb-accommodated dislocation-creep.

The variable mantle widths observed on feldspar augen in ultramylonite are probably related to the relative rate of recrystallization vs rotation rate of the augen (Passchier & Simpson 1986). Recrystallized mantles are small where either (i) dynamic recrystallization rate is low or (ii) the rate of porphyroclast rotation is high. The proportion of matrix in a mylonite increases as dynamically-recrystallized grains are displaced from the parent grain and incorporated into the matrix.

Myrmekite is ubiquitous on K-feldspar grain boundaries that are oriented parallel to the *S*-foliation (e.g. Fig. 5a) which is consistent with the observations of Simpson (1985). The composition of the plagioclase in the myrmekite (i.e. oligoclase) is generally the same composition as other plagioclase grains in the sample, including some of the recrystallized grains that surround K-feldspar augen. Some of these new grains have been produced by the dynamic recrystallization of myrmekite either during or after its formation on the K-feldspar boundary. Since both well-formed myrmekite and recrystallized-grains of the same composition can occur on a single K-feldspar grain (Fig. 5c), the processes responsible for producing these microstructures must have operated synchronously.

Zone 3 is the transition zone in which feldspar microstructures indicate (i) recovery on the southeast boundary and (ii) strain hardening and cataclastic failure on the northwest. On the southeast boundary, mantled feldspar augen have highly serrated grain boundaries. The composition of new grains on these boundaries may be the same as the core grain. More commonly they are albite. Both grain-boundary migration and neocrystallization are then the mechanisms by which new grains form. The accessibility of albite-rich fluids is the most likely control on which recover mechanism was active. The new grains found along the Type-2 segregation bands in plagioclase on the southeast boundary of zone 3 (Fig. 7d) are also the result of neocrystallization. Hanmer (1982) inferred that they indicate a brittle–plastic transition for feldspars, defined here as approximately the lower temperature limit of dislocation-creep.

Neocrystallization similar to that shown in Fig. 7(a) has been described by Allison *et al.* (1979) from other mylonites produced under retrograde metamorphic conditions. The apparent superplasticity they observed in the mylonites was attributed to the process of neocrystallization, which is thought to be an example of transformation plasticity. Perhaps it is not coincidental that grain-size reduction by neocrystallization occurs in the zone in this study that has the highest differential displacement, indicated by the largest metamorphic gradient in the area.

Microkinks, kink bands and flame perthite

Microkinks (e.g. Fig. 5b) are common in both K-feldspar and plagioclase in zone 3 even in the absence of abundant grain-scale faulting. Tullis & Yund (1987) determined that microkinks in experimentally deformed feldspars form by cataclastic failure at sites of dislocation tangles. Microkinks, therefore, indicate deformation by cataclastic flow. The rare microkinking observed in zone 4, only in K-feldspar (Fig. 6b), is most likely due to pinning of dislocations at microperthitic lamellae. It may also cause strain hardening and lead to subgrain-scale microfaults in the same grains (Fig. 6b, small arrow). Thus, while recovery-accommodated dislocation-glide occurred to the southeast side of zone 3 (parallel to isograd C; Fig. 3), no recovery was possible northwest of that boundary. The rarity of microkinks and deformation bands occurring on the northwest side of zone 3 indicates that dislocation glide was difficult. The northwest boundary of zone 3 would therefore correspond to the limit of dislocation climb in feldspar, which occurs at approximately 450°C (Tullis & Yund 1980).

Angular relationships presented for kink-bands in plagioclase from zone 4 (Fig. 6a) indicate that the formation of these kink-bands is controlled by twin-gliding. The abundance of mechanical twins and kink bands indicates that a significant amount of twin-gliding occurred in plagioclase. Abundant glide-twins and kink bands in zone 3 attest to the continued activity of twin-gliding (Fig. 8b) as dislocation movement became difficult. This is to be expected since the production of glide-twins is independent of temperature and require only the application of a differential stress in plagioclase with greater than 10% An (Tullis 1980). In zone 2, microstructures indicative of dislocation-glide are not found; the bent twins and undulatory extinction observed are assumed to result from an array of microcracks rather than dislocations (Tullis & Yund 1977). The prominent glide-twins in these fractured feldspars both pre- and post-date shear fractures (Fig. 8c) and must therefore be syntectonic.

Flame perthite (Figs. 7c & d) occurs in zones 2 and 3. Generally, flames have a preferential orientation parallel to the inferred maximum stress direction. The appearance of flame perthite in zone 3 correlates with both the transition to brittle behaviour in feldspar and the alteration of plagioclase to albite + epidote. Flame perthite is a replacement texture resulting from the breakdown of plagioclase during deformation under conditions of retrograde metamorphism with an imposed differential stress (Pryer & Robin 1991). A detailed presentation of this model is in preparation.

Brittle microstructures

Microfractures in zone 5 and the localized polysynthetic twins in K-feldspar that highlight the fractures are assumed to be a late feature imposed during uplift to higher crustal levels, resulting from either interaction with water (Tullis & Yund 1980, Tullis 1983) or extension due to unloading. Because of the plasticity implied by the microstructures in this zone, the more brittle microstructures must have been superimposed on the plastic microstructures or they would have been destroyed during progressive deformation (Tullis 1983, Tullis & Yund 1987). In general, microfractures observed in zone 4 have a tendency to concentrate parallel to the *S*-foliation direction (Fig. 10), suggesting that the majority of these fractures formed as extension fractures due to unloading.

Beginning at the northwest boundary of zone 3 and continuing throughout zone 2, feldspar deformation is dominated by brecciation and fragment displacement. Grain-size reduction in mylonites is accomplished through continued fracturing in grains and on grain boundaries. Compositional banding of quartz and feldspar in the mylonites suggests that all grains along any given string have been derived from the same parent grain (Fig. 8a). Even representation over a wide range in feldspar grain-size is indicative of deformation by cataclastic milling.

Synthetic shear fractures dominate in zone 3 (Fig. 10). Complete separation of fragments on synthetic fractures such as those in Fig. 8(b), and continued antithetic rotation of the individual fragments results in feldspar 'fish' (Mawer 1987, cf. Lister & Snoke 1984). In zone 2, the dominant sense of fracture displacement changes gradationally from synthetic to antithetic and therefore individual fragment rotation changes from antithetic to synthetic. This change in dominant displacement sense from synthetic to antithetic correlates with a decrease in metamorphic grade. A preliminary model for the control on the dominant sense of displacement is presented in Pryer (1992).

Zone 1 is characterized by the cataclastic deformation of both quartz and feldspar. The temperature at the time of deformation must therefore have been well below that necessary for recovery in quartz.

SUMMARY

In zones 4 and 5, dynamic recrystallization through either subgrain rotation or grain boundary migration occurs in feldspars. Petrological evidence combined with the observation by others (e.g. Olsen & Kohlstedt 1985) of recovery by dynamic recrystallization in naturally deformed rocks, indicate that deformation probably took place at temperatures greater than 550°C. On the southeast side of zone 3, recrystallization through the nucleation and growth of new grains at grain boundaries or in segregation bands is the dominant mechanism. Fracturing of feldspars is of minor importance.

Cataclastic failure of feldspars dominates the mode of deformation from central zone 3 to the northwest limit of mapping. This change in mode of deformation, marked by the limit of dislocation climb in feldspars, occurs in conjunction with the disappearance of hornblende, the repacement of oligoclase by albite + epidote and the appearance of flame perthite. It correlates with the change from lower amphibolite to upper greenschist grade conditions, between 450 and 500°C. The size of fractures and their importance as a deformation mechanism increases from southeast to northwest. Southeast of zone 3 fractures are generally minute and insignificant whereas within the JLSZ and continuing to the northwest, grain-scale faults and fractures completely dominate the strain in feldspars.

Along the northwest boundary of zone 3 grain-scale faults with synthetic displacement are the dominant mode of deformation in combination with deformation twins, undulatory extinction, deformation bands and kink bands. Within the central portion of zone 2 the mode of deformation is dominated by grain-scale faults with antithetic displacement. The predominance of antithetic fractures in central zone 2, combined with observations made by others (White 1975, Boullier 1980), indicates that temperatures were probably between 300 and 400°C. Between the northern part of zone 2 and the northwest limit of mapping, the randomly oriented fracturing in feldspar and the cataclastic failure of quartz indicate that temperatures during deformation were below 300°C.

The observations from this study of microstructures in rocks deformed naturally at different metamorphic grades indicate that the microstructures produced and the changes in microstructures with changing temperature, pressure, P_{H_2O} and strain-rate, can be compared to those observed in experimentally deformed rocks. It is also reasonable to propose that microstructures can be used to indicate the metamorphic grade at which deformation took place.

Acknowledgements—I would like to thank P. M. Clifford (McMaster University), A. Davidson (Geological Survey of Canada) and N.S.E.R.C. for supervision and/or financial support during the collection of preliminary data; P.-Y. F. Robin (University of Toronto) and N.S.E.R.C. for support of the Ph.D. thesis during which this was written; P. M. Clifford, P.-Y. F. Robin, C. K. Mawer, A. C. Cruden and the members of a University of Toronto graduate course for their comments on earlier versions of the manuscript; S. F. Wojtal, J. Tullis and two anonymous reviewers for very helpful criticisms and comments; and P.-Y. Robin, J. Tullis and J. C. White for enlightening discussions which, along with the reviews, have resulted in significant improvements to the manuscript. Any errors or misinterpretations are entirely my own.

REFERENCES

Allison, I., Barnett, R. L. & Kerrich, R. 1979. Superplastic flow and changes in crystal chemistry of feldspars. *Tectonophysics* **53**, T41–T46.

Boullier, A.-M. 1980. A preliminary study on the behavior of brittle minerals in a ductile matrix: example of zircons and feldspars. *J. Struct. Geol.* **2**, 211–217.

Boullier, A.-M. & Bouchez, J.-L. 1978. Le quartz en rubans dans les mylonites. *Bull. Soc. géol. Fr.* **20**, 253–262.

Davidson, A. 1986. Grenville Front relationships near Killarney, Ontario. In: *The Grenville Province* (edited by Moore, J. M., Davidson, A. & Baer, A. J.). *Spec. Pap. Geol. Ass. Can.* **31**, 107–118.

Davidson, A., Nadeau, L., Grant, S. M. & Pryer, L. L. 1985. Studies in the Grenville Province of Ontario. *Geol Surv. Pap. Can.* **85-1A**, 463–483.

Derry, D. R. 1950. A tectonic map of Canada. *Proc. geol. Ass. Can.* **3**, 39–53.

Frarey, M. J. & Cannon, R. T. 1969. Notes to accompany a map of the geology of the Proterozoic rocks of the Lake Panache–Collins Inlet map areas, Ontario. (41I/3, H/14). *Geol. Surv. Pap. Can.* **68-63**.

Fuhrman, M. L. & Lindsley, D. H. 1988. Ternary feldspar modelling and thermometry. *Am. Mineral.* **73**, 201–215.

Ghosh, S. K. & Ramberg, H. 1976. Reorientation of inclusions by combination of pure and simple shear. *Tectonophysics* **34**, 1–70.

Hanmer, S. 1982. Microstructure and geochemistry of plagioclase and microcline in naturally deformed granite. *J. Struct. Geol.* **4**, 197–213.

Jensen, L. N. & Starkey, J. 1985. Plagioclase microfibres in a ductile shear zone from the Jotun Nappe, Norway. *J. Struct. Geol.* **7**, 527–539.

La Tour, T. E. & Fullagar, P. D. 1986. Rb–Sr study of mylonitic rocks at the Grenville Front near Coniston, Ontario: some preliminary results. In: *The Grenville Province* (edited by Moore, J. M., Davidson, A. & Baer, A. J.). *Spec. Pap. Geol. Ass. Can.* **31**, 223–233.

Lister, G. S. & Snoke, A. W. 1984. S–C mylonites. *J. Struct. Geol.* **6**, 617–638.

Mawer, C. K. 1987. Shear criteria in the Grenville Province, Ontario, Canada. *J. Struct. Geol.* **9**, 531–539.

O'Donnell, L. L. 1986. Characterization of the nature of deformation and metamorphic gradient across the Grenville Front Tectonic Zone in Carlyle Township, Ontario. Unpublished M.Sc. thesis, McMaster University, Hamilton, Ontario.

Olsen, T. S. & Kohlstedt, D. L. 1985. Natural deformation and recrystallization of some intermediate plagioclase feldspars. *Tectonophysics* **111**, 107–131.

Passchier, C. W. 1985. Water-deficient mylonite zones—an example from the Pyrenees. *Lithos* **18**, 115–127.

Passchier, C. & Simpson, C. 1986. Porphyroclast systems as kinematic indicators. *J. Struct. Geol.* **8**, 831–843.

Pryer, L. L. 1985. Preliminary report on the Grenville Front Tectonic Zone, Carlyle Township, Ontario. *Geol. Surv. Pap. Can.* **85-1A**, 463–483.

Pryer, L. L. 1992. A model for the transition from antithetic to synthetic displacement on grain-scale faults in greenschist-grade mylonites with increasing metamorphic grade. *Wolfville '92, GAC-MAC Joint Annual Meeting, Prog. w. Abs.* **17**.

Pryer, L. L. & Robin, P.-Y. F. 1991. A model for albite flame growth, *TERRA Abs.* 5 (Suppl. to *TERRA Nova* 3, 32).

Robin, P.-Y. F. & Jowett, E. C. 1986. Computerized density contouring and statistical evaluation of orientation data using counting circles and continuous weighting functions. *Tectonophysics* **121**, 207–223.

Simpson, C. 1985. Deformation of granitic rocks across the brittle–ductile transition. *J. Struct. Geol.* **7**, 503–511.

Simpson, C. & Wintsch, R. P. 1989. Evidence for deformation-induced K-feldspar replacement by myrmekite. *J. metamorph. Geol.* **7**, 261–275.

Smith, J. V. 1974. *Feldspar Minerals, Volume* 2. Springer, New York.

Smith, J. V. & Brown, W. L. 1988. *Feldspar Minerals, Volume* 1. Springer, New York.

Stockwell, C. H. 1982. Proposals for time classification and correlation of Precambrian rocks and events in Canada and adjacent areas of the Canadian Shield; Part 1: A time classification of Precambrian rocks and events. *Geol. Surv. Pap. Can.* **80-19**.

Tullis, J. 1978. Mylonites—natural and experimental; Processes and conditions of mylonite formation as inferred from experimental deformation studies. *Geol. Soc. Am. Short Course Notes*, 7–8 March 1978, Boston, Massachusetts.

Tullis, J. 1983. Deformation of feldspars. In: *Feldspar Mineralogy* (2nd edn) (edited by Ribbe, P. H.). *Miner. Soc. Am. Rev. Mineral.* **2**, 297–323.

Tullis, J. & Yund, R. A. 1977. Experimental deformation of dry Westerly granite. *J. geophys. Res.* **82**, 5705–5718.

Tullis, J. & Yund, R. A. 1980. Hydrolitic weakening of experimentally deformed Westerly granite and Hale albite rock. *J. Struct. Geol.* **2**, 439–451.

Tullis, J. & Yund, R. A. 1987. Transition from cataclastic flow to dislocation creep of feldspar: mechanisms and microstructures. *Geology* **15**, 606–609.

Tullis, T. E. 1980. The use of mechanical twinning in minerals as a measure of shear stress magnitudes. *J. geophys. Res.* **85**, 6263–6268.

van Breeman, O. & Davidson, A. 1988. Northeast extension of Proterozoic terrains of mid-continental North America. *Bull. geol. Soc. Am.* **100**, 630–638.

Vidal, J.-L., Kubin, L., Debat, P. & Soula, J.-C. 1980. Deformation and dynamic recrystallization of K-feldspar augen in orthogneiss from Montagne Noire, Occitania, Southern France. *Lithos* **13**, 247–255.

White, J. C. & White, S. H. 1983. Semi-brittle deformation within the Alpine fault zone, New Zealand. *J. Struct. Geol.* **5**, 579–589.

White, S. 1975. Tectonic deformation & recrystallization of oligoclase. *Contr. Miner. Petrol.* **50**, 287–304.

Wynne-Edwards, H. R. 1972. The Grenville Province. In: *Variations in Tectonic Styles in Canada* (edited by Price, R. A. & Douglas, R. J. W.). *Spec. Pap. Geol. Ass. Can.* **11**, 263–334.

Yund, R. A. & Tullis, J. 1991. Compositional changes of minerals associated with dynamic recrystallization. *Contr. Miner. Petrol.* **108**, 346–355.